
This is an electronic reprint of the original article.

This reprint may differ from the original in pagination and typographic detail.

Askola, J.; Maham, K.; Kärh , Petri; Ikonen, E.

Increased detector response in optical overfilled measurements due to gas lens formation by nitrogen flow through the entrance aperture

Published in:
Metrologia

DOI:
[10.1088/1681-7575/ac0e7b](https://doi.org/10.1088/1681-7575/ac0e7b)

Published: 01/10/2021

Document Version
Publisher's PDF, also known as Version of record

Published under the following license:
CC BY

Please cite the original version:
Askola, J., Maham, K., K rh , P., & Ikonen, E. (2021). Increased detector response in optical overfilled measurements due to gas lens formation by nitrogen flow through the entrance aperture. *Metrologia*, 58(5), Article 055008. <https://doi.org/10.1088/1681-7575/ac0e7b>

PAPER • OPEN ACCESS

Increased detector response in optical overfilled measurements due to gas lens formation by nitrogen flow through the entrance aperture

To cite this article: J Askola *et al* 2021 *Metrologia* **58** 055008

View the [article online](#) for updates and enhancements.

Increased detector response in optical overfilled measurements due to gas lens formation by nitrogen flow through the entrance aperture

J Askola^{1,*}, K Maham¹, P Kärhä¹ and E Ikonen^{1,2}

¹ Metrology Research Institute, Aalto University, Espoo, Finland

² VTT MIKES, VTT Technical Research Centre of Finland Ltd, Espoo, Finland

E-mail: janne.askola@aalto.fi

Received 15 March 2021, revised 7 June 2021

Accepted for publication 24 June 2021

Published 23 August 2021



Abstract

According to our experimental results, a nitrogen flow used to prevent dust and moisture entering a detector may influence measurements performed with trap detectors in overfilled conditions. A stable light source was measured with a wedged trap detector with 4 mm aperture, and the nitrogen flow rate was varied. The nitrogen flow was found to have the largest effect of up to 0.8% on the responsivity of the detector at around 1.0 l min^{-1} flow rate. The effect of nitrogen flow can be removed down to 0.02% by an added crossflow which removes the nitrogen out of the optical axis. In another experiment, the effect was removed almost completely by changing the flowing gas from nitrogen to synthetic dry air. We also present measurement results that indicate the responsivity changes with nitrogen to be smaller than 0.05% with underfilled beam geometry, even without the added crossflow. Based on simulations, the nitrogen flow through the detector forms a gradient-index type gas lens in front of the detector increasing the effective aperture area and thus the responsivity. In the underfilled measurement geometry there is no light close to the aperture edge which could be refracted inside the detector. Finally, we consider methods to ensure that the responsivity changes due to the gas flow remain below 0.05% in overfilled measurement geometry, without compromising the cleanliness of the detector with too small gas flow rate.

Keywords: trap detector, nitrogen purge, overfill mode, gas lens effect, crossflow

(Some figures may appear in colour only in the online journal)

1. Introduction

In photometry and radiometry, trap detectors are commonly used as transfer standard detectors of optical power [1–4]. Reflected laser beam from the first photodiode of a trap

detector can be collected with subsequent photodiodes in specific geometrical arrangements. For the highest accuracy, the photodiodes are used without any protective windows, and thus exposed to ambient conditions of the laboratory. The possible dust and moisture accumulation on the photodiodes needs to be taken into account increasing the uncertainty in the measurements, and shortening the calibration interval. In contrast to single photodiode detectors with protective windows, removal of contamination from the photodiodes of trap detectors is challenging because of limited space available within the tight geometrical arrangement of the photodiodes.

* Author to whom any correspondence should be addressed.



Original content from this work may be used under the terms of the [Creative Commons Attribution 4.0 licence](https://creativecommons.org/licenses/by/4.0/). Any further distribution of this work must maintain attribution to the author(s) and the title of the work, journal citation and DOI.

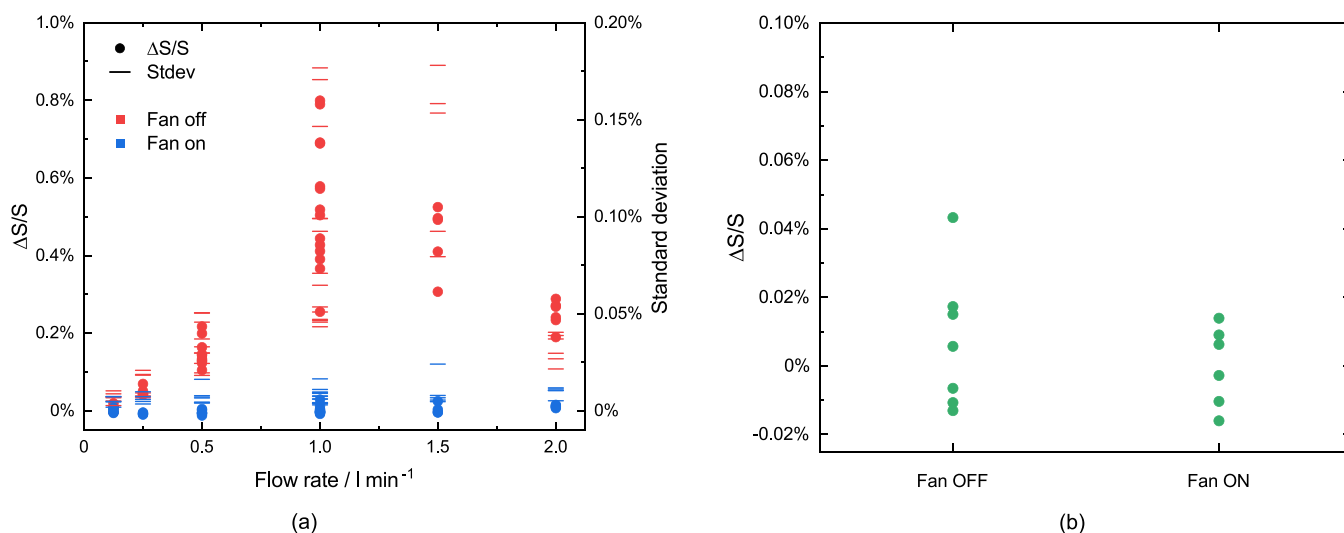


Figure 1. Relative change of photocurrents and their standard deviations when measuring a stable white LED source with a trap detector and a 4 mm diameter limiting aperture in overfilled condition (a) as a function of the nitrogen flow rate and (b) when using the flow of dry synthetic air at 1.0 l min⁻¹ in the purging. In measurements with ‘fan on’ an additional air flow perpendicular to the optical axis was applied to reduce the amount of purging gas close to the optical axis. With synthetic air, the relative change of photocurrents is almost two orders of magnitude smaller than with nitrogen flow when not using the fan.

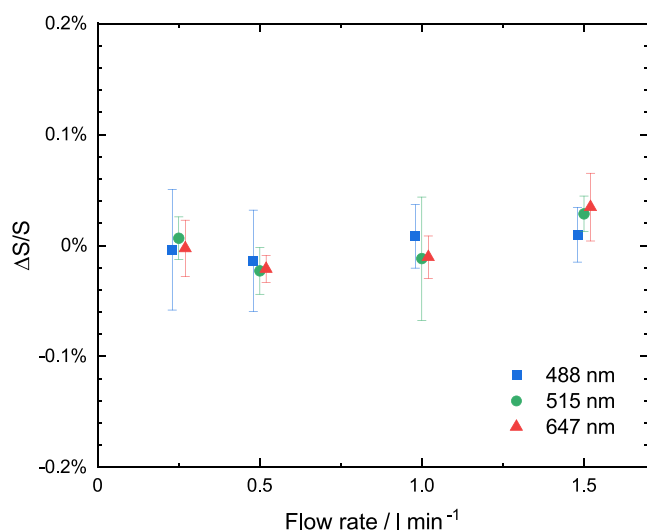


Figure 2. Relative change of photocurrents of the trap detector measured in underfilled conditions with laser beams at different wavelengths and nitrogen flow rates. An aperture of 10 mm diameter was used. Note the change of vertical scale relative to figure 1(a).

Trap detectors can be equipped with precision apertures and used in overfilled conditions to measure the irradiance or illuminance of a light source with an omnidirectional radiation pattern. Typically, a passband filter and a precision aperture are used when measuring incandescent lamps or black-body radiators [5–7]. Recently, new measurement methods for LED lamps have been introduced, where trap detectors are used to measure illuminance of LED lamps without filters [8, 9]. This has become possible, because with LEDs all radiation is within the silicon detector spectral range, but dust protection of the photodiodes is then again needed when operating in normal laboratory conditions [9].

A nitrogen flow system can be used to prevent moisture and dust collection on the photodiodes [10–13]. A constant flow of dry nitrogen is introduced through the detector, where it exits the entrance aperture preventing unwanted particles and moisture entering the detector. The optical properties of nitrogen are rather similar to those of air. Based on this, the flow should tentatively not introduce any errors into the measurements. In addition to the predictable quantum efficient detectors [10], the nitrogen flow method can be used to protect any kind of trap detectors [14].

In this paper, we present our study on the effect of nitrogen flow on the responsivity of trap detectors. Our experimental results indicate that the nitrogen flow can increase responsivity in overfilled measurement conditions. The results can be qualitatively understood on the basis of a gradient-index lens formed by the nitrogen flow in front of the detector aperture. According to those analyses we propose methods to remove possible measurement errors due to the gas flow in overfilled measurement geometry. Those methods are designed to maintain the desired protection against dust and humidity contamination of the detector.

2. Measurements

We measured the trap detector response for a 5 cm diameter LED light source with 24 separate LEDs [15] at a distance of 4.5 m using methods presented in [9]. Measurements were carried out with a wedged trap detector of two photodiodes [12] equipped with a precision aperture in overfilled conditions. The light beam diameter was more than 100 times the 4 mm diameter of the aperture. The integration time for a single measurement was 0.2 s. Figure 1 presents the changes of photocurrents from the trap detector at nominal nitrogen flow rates of 0.125–2.0 l min⁻¹ and synthetic air flow rate of 1.0 l min⁻¹.

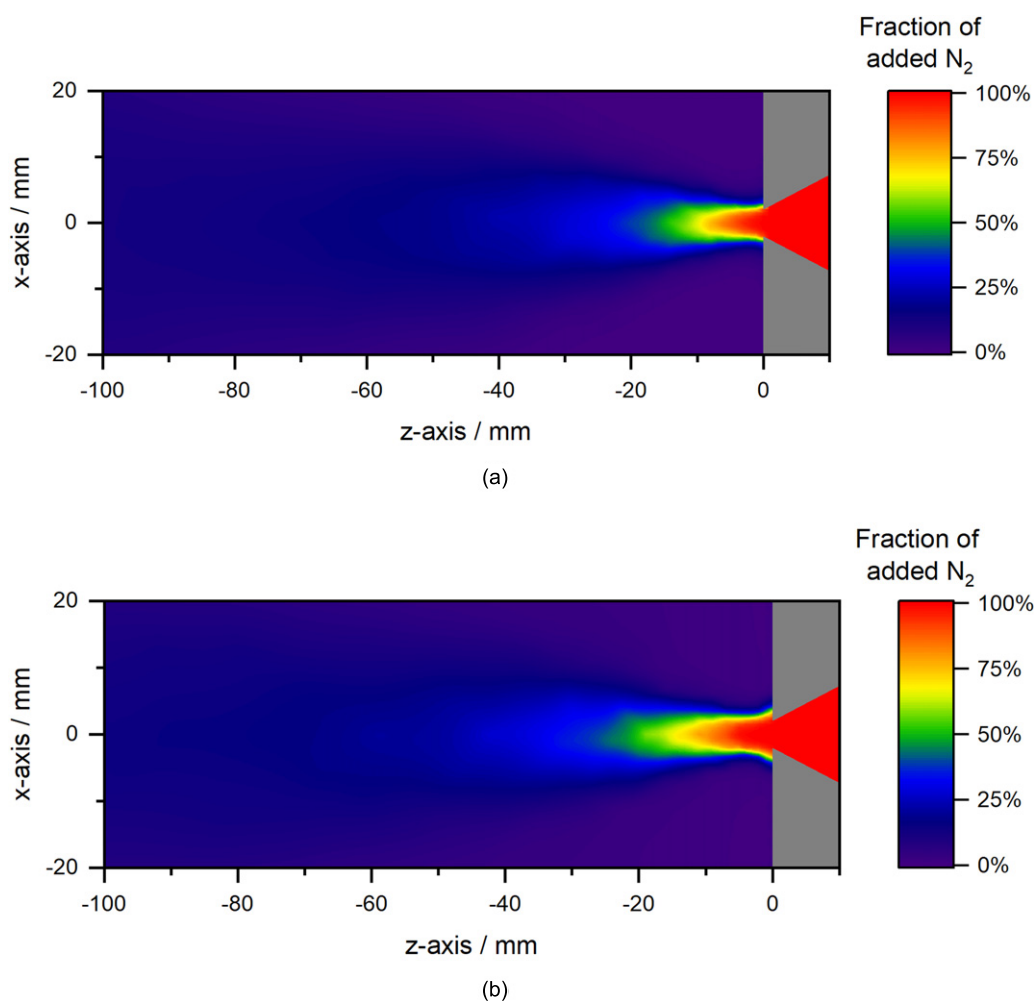


Figure 3. Simulated nitrogen flow distributions out of a detector through a 4 mm aperture with flow rates of 0.125 l min⁻¹ (a) and 1.0 l min⁻¹ (b). The length and the width of the simulated area are 100 mm and 40 mm, respectively. The simulated results are shown at the steady state of the system. The aperture of the detector is drawn with grey colour.

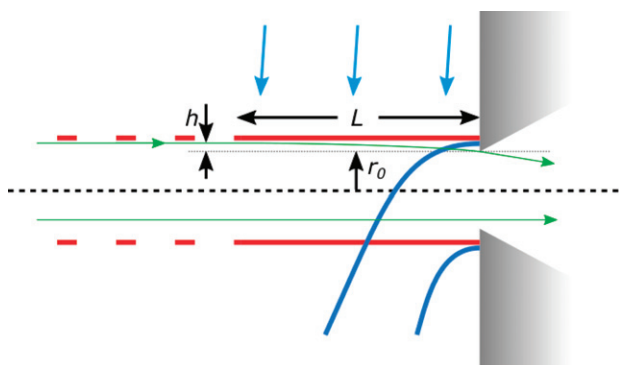


Figure 4. Model for the effects of gradient-index lens (red lines) and crossflow (blue curves and light blue arrows). Green arrows denote possible light paths. The effective length of the undisturbed lens is L , radius of the aperture is r_0 , and h indicates the maximum transverse deviation produced by the lens.

The standard deviations of each data point consisting of 10 repeated measurements are also indicated in figure 1(a). It can be noticed that with the flow rate of 1.0 l min⁻¹, both the

photocurrent values indicated by red dots and the corresponding standard deviations are at maximum.

An additional fan was then used to blow the nitrogen gas away from the optical axis. It is seen that when using the additional fan, the measurement results at all flow rates, including the results at 1.0 l min⁻¹, were within 0.02% from the measurement results at the minimum flow rate, 0.125 l min⁻¹ (blue dots in figure 1(a)). The measurements with the fan on and off were found to be consistent over a measurement period of 2 hours, during which the fan was switched on and off multiple times. The standard deviation of different measurements was 0.01% including also deviations due to the variations of the light source used.

Part of the measurements were repeated using dry synthetic air instead of nitrogen in the purging. The dry air consisted of nitrogen as the base gas and 21% of oxygen as specified by the manufacturer. The amount of other gases in the mixture was below 5 ppm. In figure 1(b), it is seen that the deviation from zero at the synthetic air flow rate of 1.0 l min⁻¹ is the same with and without the additional fan. The differences are similar as the ones observed with the lowest achieved flow rate with nitrogen purging.

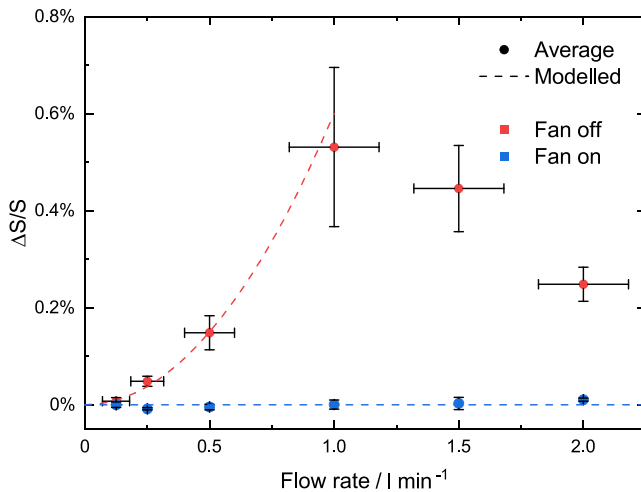


Figure 5. Relative change of photocurrents at different nitrogen flow rates. The error bars in vertical direction are standard deviation of the different measurements in figure 1(a) and in horizontal direction the standard deviation of the setting of the flow rate.

The trap detector used in the measurements was also studied for the responsivity at different laser wavelengths in under-filled mode utilizing different flow rates of nitrogen. It is anticipated on the basis of the results of figure 1 that the critical paraxial light paths are located close to the aperture edge. The purpose of these measurements was to exclude any other reasons for the increased responsivity than those related to non-zero illuminance close to the aperture edge. The normalized results are shown in figure 2, where it can be seen that the changes in responsivity are one order of magnitude smaller than the changes in the measurements made in the overfilled mode. The additional air flow by the fan was not used in these measurements.

3. Discussion

The distributions of the fraction of added nitrogen were simulated in three dimensions for different flow rates using COMSOL Multiphysics. A detector housing with an aperture diameter of 4 mm was modelled. At the beginning of the simulation, the inside of the detector housing was set to contain only nitrogen and the outside only air. Figure 3 shows the simulation results as the fraction of added nitrogen at the steady state for the flow rates of 0.125 and 1.0 l min⁻¹. It is seen that the length of the flow profile increases with higher flow rate. There is a significant increase, in particular, of the thickness in the direction of the optical axis of such a volume where the fraction of added nitrogen remains at 100% over the whole cross-sectional area corresponding to the entrance aperture.

Thermal gradients have been used to form gas lenses [16, 17]. Here the increased photocurrent of trap detector can be explained by a gradient-index lens in front of the aperture formed by the flowing nitrogen gas (see figure 4). Weighting by the spectrum of the white LED source, the average refractive index of nitrogen is larger by 6.2×10^{-6} than that of air [18]. The gradient-index lens is described by a nitrogen cylinder of length L and steep radial gradient of the

refractive index, $g = (dn/dr)|_{r=r_0} = 3 \times 10^{-5} \text{ mm}^{-1}$, where $r_0 = 2 \text{ mm}$ is the radius of the aperture. The lens increases the effective aperture area by $\Delta A = 2\pi r_0 h$, where $r_0 + h$ is the largest distance from the optical axis for which paraxial rays are deviated to pass through the aperture. With such a lens in front of the aperture, the relative change in the measured photocurrent is $\Delta S/S = \Delta A/(\pi r_0^2) = gL^2/r_0$. For the nitrogen flow rate of 0.5 l min⁻¹ and $L = 10 \text{ mm}$, the relative change of the signal is 0.15% indicating that $h = 1.5 \mu\text{m}$. The parabolic curve in figure 5 is drawn assuming that L is proportional to the nitrogen flow rate below 1.0 l min⁻¹. As a result, the area of the detector aperture effectively increases for the overfilled measurement condition. When the crossflow is used as symbolized by the light blue arrows in figure 4, the gradient-index lens effect becomes negligible for the downwards bent nitrogen flow. That is indicated by the blue dashed line in figure 5.

A flow through an orifice type of structure, in our case the optical aperture, exhibits vortex streets [19–21]. Reynolds number, defined for a circular shape as $Re = \rho v d / \mu$, where ρ is the density of the fluid, v the flow rate in m s⁻¹, d the diameter of the orifice, and μ the viscosity of the fluid, is used for determining the mode of the flow instability. At low Reynolds numbers, flows are mainly laminar. Between the Reynolds numbers of 177 and 437, corresponding to our flow rates of 0.5 and 1.25 l min⁻¹, the flow after the laminar part transforms from sinuous motion to helical shape and eventually to turbulent flow [22]. Also, the increasing flow rate, and at the same time the increasing Reynolds number, will shorten the laminar part of the flow. Our simulations were only able to produce the laminar part of the flows and it is probable that in the real nitrogen flow at high flow rates there are vortex-type microstructures which affect light propagation in the same way as scintillation in atmosphere [23, 24]. The flow stays laminar close to Reynolds numbers of 100 when using a crossflow [25], similar to the situation with the additional fan in our experiments. Based on these considerations, we describe the responsivity increase with increasing nitrogen flow rate in figure 5 to be due to the gradient-index lens which starts to reduce in length at flow rates above 1 l min⁻¹. In addition, the microstructures in the flow may cause the highest fluctuations of the photocurrent at the flow rates of 1 to 1.5 l min⁻¹.

4. Conclusions

Based on our measurements, the nitrogen flow used for purging affects the response of trap detectors in overfill conditions by up to 0.8%. Nitrogen produces a converging gradient-index gas lens. The fluctuating light intensity is possibly caused by vortex-type microstructures in the flow pattern. Simulated nitrogen flow profiles were used to estimate the effect of the gas lens on the effective aperture area of the detector. The photocurrent could be stabilized, and the effect of the gas lens removed by two methods: (i) another flow perpendicular to the optical axis to blow the nitrogen away from the light path and (ii) changing the purging gas from nitrogen to dry synthetic air.

The studied gas lens effect can appear also in other measurement setups where gas purging through an aperture is used. In some blackbody radiators, for example, argon or neon are used as inert gas, and the gas flows out of the radiator output. However, in such setups the aperture area is usually larger than the 4 mm diameter aperture in our setup and therefore, the relative change of the effective aperture area is expected to be smaller than the one observed in our measurements.

In cases where a flow of nitrogen is used to protect the detector from humidity and dust, we recommend that a flow rate of clean gas of at least 0.5 l min^{-1} should be used with a suitable crossflow in overfilled measurements. The crossflow should be adjusted so that it minimizes the probability of dust particles entering the detector. The setup with a 4 mm diameter aperture can be validated by observing that there are no responsivity changes at nitrogen gas flow rates between 0.5 and 2.0 l min^{-1} . With the use of dry synthetic air, the gas lens formation in front of the detector can be avoided. Though, the purity of the clean air used needs to be ensured because the manufacturer specifications for scientific grade nitrogen are often better. For measurement setups using nitrogen, a suitable combination of gas and flow rate and possible crossflow design need to be determined separately. These principles should ensure that the gas flow effects on trap detector responsivity in overfilled measurement conditions remain below 0.05%, which is sufficient for photometric measurements.

Acknowledgments

The work leading to this study is partly funded by the European Metrology Programme for Innovation and Research (EMPIR) Project 15SIB07 PhotoLED ‘Future Photometry Based on Solid State Lighting Products’. The EMPIR programme is co-financed by the Participating States and from the European Union’s Horizon 2020 research and innovation programme. This work is partly funded by the Academy of Finland Flagship Programme, Photonics Research and Innovation (PREIN), Decision Number: 320167. The authors would like to thank Petr Kliment for fruitful discussions about the effect of nitrogen flow on their measurements.

ORCID iDs

J Askola  <https://orcid.org/0000-0003-3267-7967>

K Maham  <https://orcid.org/0000-0001-6740-1317>

P Kärhä  <https://orcid.org/0000-0002-4774-7887>

References

- [1] Zalewski E F and Duda C R 1983 Silicon photodiode device with 100% external quantum efficiency *Appl. Opt.* **22** 2867–73
- [2] Fox N P 1991 Trap detectors and their properties *Metrologia* **28** 197
- [3] Kärhä P, Lassila A, Ludvigsen H, Manoocheri F, Fagerlund H and Ikonen E 1995 Optical power and transmittance measurements and their use in detector-based realization of the luminous intensity scale *Opt. Eng.* **34** 2611–8
- [4] Kūbarsepp T, Kärhä P and Ikonen E 1997 Characterization of a polarization-independent transmission trap detector *Appl. Opt.* **36** 2807–12
- [5] Kūbarsepp T, Kärhä P, Manoocheri F, Nevas S, Ylianttilä L and Ikonen E 2000 Spectral irradiance measurements of tungsten lamps with filter radiometers in the spectral range 290 nm to 900 nm *Metrologia* **37** 305
- [6] Kärhä P, Harrison N J, Nevas S, Hartree W S and Abu-Kassem I 2003 Intercomparison of characterization techniques of filter radiometers in the ultraviolet region *Metrologia* **40** S50
- [7] Taubert D R, Friedrich R, Hartmann J and Hollandt J 2003 Improved calibration of the spectral responsivity of interference filter radiometers in the visible and near infrared spectral range at PTB *Metrologia* **40** S35
- [8] Dönsberg T, Pulli T, Poikonen T, Baumgartner H, Vaskuri A, Sildoja M, Manoocheri F, Kärhä P and Ikonen E 2014 New source and detector technology for the realization of photometric units *Metrologia* **51** S276
- [9] Pulli T, Dönsberg T, Poikonen T, Manoocheri F, Kärhä P and Ikonen E 2015 Advantages of white LED lamps and new detector technology in photometry *Light: Sci. Appl.* **4** e332
- [10] Sildoja M et al 2013 Predictable quantum efficient detector: I. Photodiodes and predicted responsivity *Metrologia* **50** 385
- [11] Müller I et al 2013 Predictable quantum efficient detector: II. Characterization and confirmed responsivity *Metrologia* **50** 395
- [12] Dönsberg T, Sildoja M, Manoocheri F, Merimaa M, Petroff L and Ikonen E 2014 A primary standard of optical power based on induced-junction silicon photodiodes operated at room temperature *Metrologia* **51** 197
- [13] Salfner K, Dönsberg T, Porrovecchio G, Smid M, Nield K and Nevas S 2018 Characterization of a room temperature predictable quantum efficient detector for applications in radiometry and photometry *Metrologia* **55** 654
- [14] L-1 Standards and Technology, Inc. 2013 Model LTD-10: 3-element trap detector, S/N LTD-10-134, user manual <http://l-1.biz/assets/ltd-11-trap-detector-manual.pdf>
- [15] Luminous intensity GbR 2020 LIS-A, luminous intensity standard <https://luminous-intensity.de> (accessed 10 March 2020)
- [16] Berreman D W 1964 B. S. T. J. briefs: a lens or light guide using convectively distorted thermal gradients in gases *Bell Syst. Tech. J.* **43** 1469–75
- [17] Aoki Y and Suzuki M 1967 Imaging property of a gas lens *IEEE Trans. Microw. Theory Tech.* **15** 2–8
- [18] Zhang J, Lu Z H and Wang L J 2008 Precision refractive index measurements of air, N₂, O₂, Ar, and CO₂ with a frequency comb *Appl. Opt.* **47** 3143–51
- [19] Johansen F C 1930 Flow through pipe orifices at low Reynolds numbers *Proc. R. Soc. A* **126** 231–45
- [20] Crow S C and Champagne F H 1971 Orderly structure in jet turbulence *J. Fluid Mech.* **48** 547–91
- [21] Gohil T B, Saha A K and Muralidhar K 2012 Numerical study of instability mechanisms in a circular jet at low Reynolds numbers *Comput. Fluids* **64** 1–18
- [22] Kwon S J and Seo I W 2005 Reynolds number effects on the behavior of a non-buoyant round jet *Exp. Fluids* **38** 801–12
- [23] Sofieva V F, Dalaudier F and Vernin J 2013 Using stellar scintillation for studies of turbulence in the Earth’s atmosphere *Phil. Trans. R. Soc. A* **371** 20120174
- [24] Vetelino F S, Clare B, Corbett K, Young C, Grant K and Andrews L 2006 Characterizing the propagation path in moderate to strong optical turbulence *Appl. Opt.* **45** 3534–43
- [25] Camussi R, Guj G and Stella A 2002 Experimental study of a jet in a crossflow at very low Reynolds number *J. Fluid Mech.* **454** 113